JOURNAL OF MATERIALS RESEARCH AND TECHNOLOGY 2023;24:7040–7046

Available online at www.sciencedirect.com

jmr&t Journal of Materials Research and Technology

journal homepage: www.elsevier.com/locate/jmrt

Short Communication

# Tailoring the surface characteristic of metallic glass for wettability control

Yongfeng Qian [a], Hanlin Liu [a], Lin Zhang [b], Minqiang Jiang [c,d], Hu Huang [a,*], Jiwang Yan [b]

[a] Key Laboratory of CNC Equipment Reliability, Ministry of Education, School of Mechanical and Aerospace Engineering, Electron Microscopy Center, Jilin University, Changchun, Jilin 130022, China

[b] Department of Mechanical Engineering, Faculty of Science and Technology, Keio University, Yokohama 223-8522, Japan

[c] State Key Laboratory of Nonlinear Mechanics, Institute of Mechanics, Chinese Academy of Sciences, Beijing 100190, China

[d] School of Engineering Science, University of Chinese Academy of Sciences, Beijing 100049, China

ARTICLE INFO

Article history:
Received 16 February 2023
Accepted 1 May 2023
Available online 5 May 2023

Keywords:
Metallic glass
Wettability
Laser patterning
Heat treatment
Gradient wetting
Extreme wetting contrast

ABSTRACT

Bulk metallic glasses (BMGs) have attracted broad research interest in industrial and commercial fields due to their outstanding mechanical and physical properties. Achieving controlled manipulation of their surface wettability is expected to further improve their applicability. In this study, the functional MG surfaces with various wetting behaviors (including superhydrophilicity, superhydrophobicity, gradient wettability, coexistence of superhydrophilicity and superhydrophobicity) were fabricated by controlling the surface microstructure and chemical composition, which were achieved by laser processing and low-temperature heat treatment. The laser-patterned MG surface with hierarchical micro/nanostructures showed hydrophilicity, and it turned to hydrophobicity after heat treatment, which could be attributed to the adsorption of organic matter from the ambient air. The fabricated gradient wetting surface achieved directional transport of droplets, and the constructed extreme wetting contrast surface exhibited good ability in controlling the spreading of droplets.



## 1. Introduction

Nature-inspired hierarchical structured surfaces with extreme wettability play a pivotal role in daily activities, industrial and biological applications. For instance, superhydrophilic surfaces have positive effects on heat transfer [1,2] and biomolecular immobilization [3], while superhydrophobic surfaces exhibit broad prospects in anti-icing [4,5], anti-biofouling [6], microfluid manipulation [7] and energy-related applications [7]. Although superhydrophilic/superhydrophobic

* Corresponding author.
E-mail address: huanghu@jlu.edu.cn (H. Huang).

https://doi.org/10.1016/j.jmrt.2023.05.004

surfaces appear to be promising, they are generally fabricated on polymers with low mechanical stability [8–11], which may be easily damaged in harsh service environments. In contrast, metallic materials with better mechanical properties may be more suitable for practical engineering applications. As ideal metallic materials for micro/nanomanufacturing, metallic glasses (MGs) are free from microstructural defects such as grain boundaries and dislocations [12–14], which endow them with superior mechanical durability and outstanding corrosion resistance [15–17]. Benefiting from these advantages, MGs are considered as one of the most desirable materials for constructing biological and structural components [18,19]. Meanwhile, achieving controlled manipulation of their surface wettability is expected to further improve their applicability, such as preparing orthopedic implants with excellent biocompatibility and developing aerospace equipment with anti-icing performance. Therefore, how to modify the surface wettability of MGs has become an urgent and necessary task.

In general, the wetting behavior of solid surfaces is strongly related to their geometrical structure and chemical composition. Taking advantage of superior ability in controlling the geometrical patterns of the surface microstructure [20–23], laser patterning technique has been widely applied to fabricate functional MG surfaces with various wetting behaviors. For example, by laser processing in an atmospheric environment, typical groove patterns were prepared on a Zr-based MG substrate, which enhanced the hydrophilicity compared to the original MG surface [24]. In addition, by low-temperature heat treatment of the laser processed MG surface, its wettability could be switched from superhydrophilicity to superhydrophobicity [25,26]. More recently, by combining laser processing and silanization modification, we successfully fabricated superhydrophobic MG surfaces, which could be attributed to the combined effects of laser-induced surface microstructure and surface chemical composition [27]. Although the above studies have effectively changed the surface wetting behavior of MGs, none of them have achieved precise wetting manipulation. Moreover, most of the current research focuses on the preparation of homogeneous wettable surfaces with stable superhydrophilic or superhydrophobic state, and it still remains a great challenge to utilize the laser-based methods to construct heterogeneous wetting surfaces, such as wetting gradient surfaces and extreme wettability contrast surfaces, especially on MG substrates. The objective of the present study is to fabricate MG surfaces with various wetting behaviors (including superhydrophilicity, superhydrophobicity, gradient wettability, coexistence of superhydrophilicity and superhydrophobicity) by controlling the surface microstructure and chemical composition, which are achieved by combining laser processing and heat treatment without using any chemicals. This study provides an insight into the relationship between macroscopic wetting behavior and microscopic surface characteristics (i.e., surface roughness and chemical composition), and guides the design strategy for functional MG surfaces with tailored wettability.

## 2. Materials and methods

The tailored MG sheets ($Zr_{41.2}Ti_{13.8}Cu_{12.5}Ni_{10}Be_{22.5}$) with dimensions of $20 \times 20 \times 2$ mm$^3$ were investigated. Prior to laser patterning, these sheets were mechanically ground and polished to a mirror finish. After mechanical polishing, the MG surface exhibits a water contact angle (CA) of 79.3° (see Fig. 5(a)), indicating the intrinsic hydrophilicity. The hierarchical MG surfaces containing patterned arrays with the scanning pitch (denoted as SP) ranging from 90 to 230 μm were prepared by using laser patterning technique (average power: 8.46 W, number of laser pulses: 1000, repetition rate: 200 kHz, pulse duration: 37 ns, central wavelength: 1064 nm, focused spot diameter: 43 μm). A fiber nanosecond pulse laser (SP–050P-A-EP-Z-F-Y, SPI Lasers) with a Gaussian beam shape was used here. After laser patterning, it was found that the micro-patterned MG surfaces were hydrophilic or even superhydrophilic. Previous studies [26,28,29] have demonstrated that low-temperature heat treatment can result in a wetting transformation from hydrophilicity to hydrophobicity on the laser-patterned metallic surfaces. Accordingly, to achieve the construction of the hydrophobic MG surfaces, the laser-patterned samples were heat treated in a thermostatic vacuum chamber (DZF-6020, Hefei Kejing Materials Technology Co., LTD) at 100 °C for 5 h.

The surface morphology and roughness of the laser-patterned samples were characterized by the scanning electron microscope (SEM, JSM-IT500A, JEOL) and laser scanning confocal microscope (LSCM, OLS4100, Olympus), respectively. The X-ray diffractometer (XRD, D8 Discover, Bruker) and X-ray photoelectron spectroscope (XPS, K-Alpha, Thermo Scientific) were employed to analyze the surface chemical composition of the laser-patterned samples. The static water CA of the laser-patterned surfaces was assessed by a CA measuring instrument (OSA60, LAUDA Scientific), and 1 μL deionized water was placed on the laser-patterned surfaces.

## 3. Results and discussion

Fig. 1(a) presents the SEM micrographs of the laser-patterned structures obtained with various SPs. It is clearly observed that periodic micro-scale protrusions are generated on the MG substrate, which are derived from the flow of molten materials driven by the recoil pressure and surface tension during the laser-MG interaction [13]. Furthermore, the high-magnification micrographs (the insets of Fig. 1(a)) reveal that the micro-protrusions are covered by many micro/nanoscale particles, which can be attributed to the ejection and re-solidification of the evaporated materials during the laser patterning process.

Fig. 1(b) presents the change in CA and roughness of the laser-patterned surface as a function of the SP value. The CAs of all the laser-patterned surfaces are significantly smaller than that of the original polished surface (79.3°), indicating that laser patterning causes the MG surfaces to become more

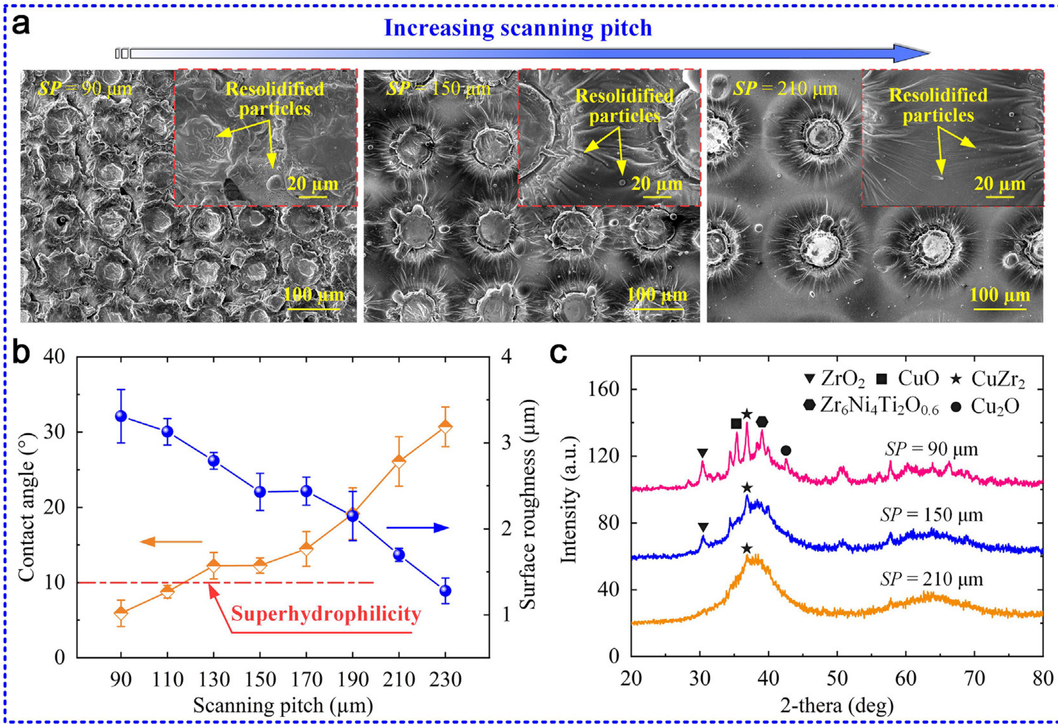


**Fig. 1 – (a) SEM micrographs of the laser-patterned structures obtained with various SPs. (b) Variations in CA and roughness of the laser-patterned surface as a function of the SP value. (c) The XRD spectrums of the laser-patterned surfaces obtained with various SPs.**

hydrophilic. In particular, the laser-patterned surfaces with SP values of 90 and 110 μm have a CA being less than 10°, showing the superhydrophilicity. In addition, the evident changes as the *SP* value decreases are that the CA gradually decreases but the surface roughness gradually increases, which indicates that the droplets on the laser-patterned surfaces satisfy the Wenzel state [30]. Apart from surface roughness, the surface chemical composition also has a crucial influence on surface wettability. The XRD spectrums displayed in Fig. 1(c) reveal that the laser-patterned surfaces with *SP* values of 90 and 110 μm consist of some metal oxides, which further contribute to the increase of surface free energy, and accordingly, resulting in an increase in surface hydrophilicity [31].

Fig. 2(a) plots the change in CA of the heat-treated laser-patterned surface as a function of the *SP* value. It is found that all the laser-patterned surfaces subjected to heat treatment show a CA being greater than 120°, confirming the effectiveness of heat treatment in converting the wettability of laser-patterned metal surfaces from hydrophilicity to hydrophobicity. In addition, the CA of the heat-treated laser-patterned surface gradually decreases from 154.3 to 124.9° when increasing the *SP* value from 90 to 230 μm, indicating that the

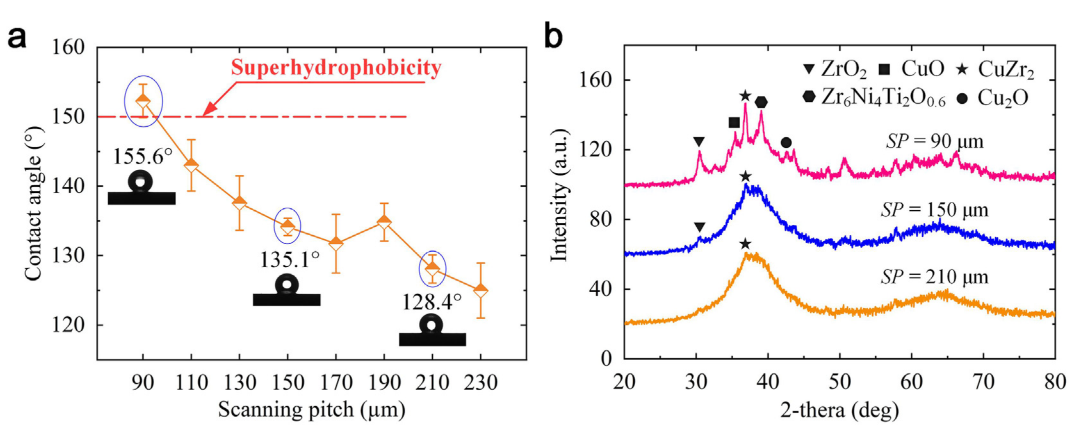


**Fig. 2 – (a) The CAs and (b) XRD spectrums of the heat-treated laser-patterned surfaces obtained with various SPs.**

heat-treated laser-patterned surface becomes more hydrophobic as the *SP* value decreases. To verify whether the phase composition of the laser-patterned surfaces is changed after heat treatment, the heat-treated laser-patterned surfaces are characterized by XRD again. The corresponding spectrums are displayed in Fig. 2(b), which exhibit consistent phase composition with those of the laser-patterned surfaces before heat treatment. This suggests that the difference in wettability of the laser-patterned surfaces before and after heat treatment is not related to the phase composition.

To explore the reasons for the significant change in wettability, the chemical composition of the laser-patterned surface before and after heat treatment is further analyzed by XPS. Figs. 3(a) and (b) show the XPS full spectrum and the corresponding elemental composition of the laser-patterned surface with *SP* of 90 μm before and after heat treatment, respectively. In Fig. 3(a), it is seen that the C (27.34%) and O (50.72%) elements are introduced into the laser-patterned surface before heat treatment, which originate from the ambient air during the laser-MG interaction. After heat treatment, an obvious change is that the content of C element increases from 27.34% to 77.99%. To confirm whether the change in wettability is related to the C group on the laser-patterned surface, the high-resolution C 1s spectrum of the laser-patterned surface before and after heat treatment is further analyzed, and the corresponding results are illustrated in Figs. 3(c) and (d), respectively. The C 1s spectrum of laser-patterned surface before and after heat treatment is divided into three peaks located at 284.8 eV, 286.3 eV and 288.5 eV, which correspond to the C–C(H), C–O and C=O groups, respectively. Among these functional groups, the non-polar C–C(H) bonds are accompanied by the hydrophobic behavior, while the polar C–O and C=O bonds increase the hydrophilicity. As shown in Figs. 3(c) and (d), the intensity of the C–C(H) group is significantly increased after heat treatment, and this may be the reason why the laser-patterned surfaces subjected to heat treatment exhibit the hydrophobicity or even superhydrophobicity. The above results demonstrate that the significant increase in hydrophobicity of the laser-patterned surfaces after heat treatment can be attributed to the adsorption of organic matter mainly including C–C(H) groups from the ambient air.

The above analysis results indicate that by adjusting the surface roughness and chemical composition, the functional MG surfaces with various homogeneous wettability could be fabricated, which provides potential support for practical engineering applications of MGs, such as biomolecular immobilization and anti-icing. Being similar to the surfaces with homogeneous wettability, gradient wetting surfaces are also highly desirable for many functional applications due to their ability to manipulate the mobility of droplets. On a gradient wetting surface, the droplet can spontaneously flow from low-wetting region to high-wetting region due to the unbalanced Laplace pressure on both sides of the droplet, as illustrated in Fig. 4(a). To achieve directional transport of droplets on the MG surface without energy input, a rectangular micro-patterned array region with gradient *SP* is designed. As shown in Fig. 4(b), the rectangular region with a length of

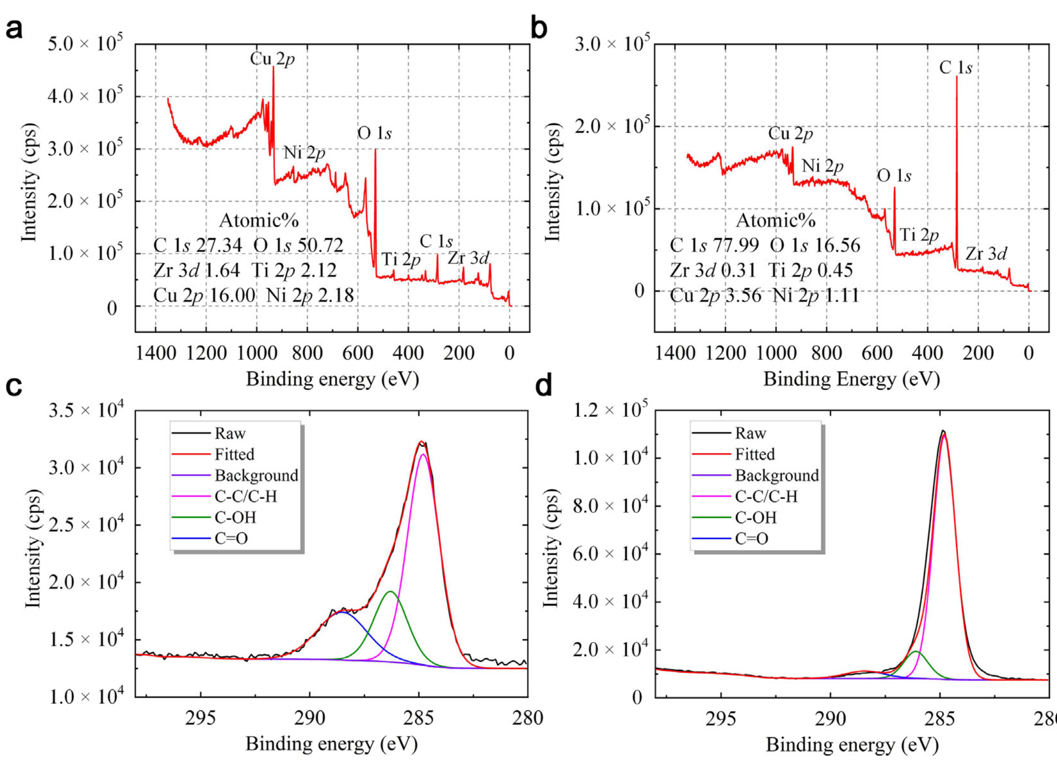


**Fig. 3 – The XPS full spectrum and the corresponding elemental composition of the laser-patterned surface obtained with *SP* of 90 μm: (a) before and (b) after heat treatment. (c) and (d) show the high-resolution C 1s spectrum of the laser-patterned surface before and after heat treatment, respectively.**

6 mm is divided equally into three parts, and the SPs of regions I, II, and III are 230, 170, and 90 μm, corresponding to the CAs of 30.7°, 14.5°, and 5.9°, respectively. Fig. 4(c) shows the final resting positions of droplets dropped on these three regions. It is found that the droplets falling on the region I or region II move towards the region III, while the droplets falling on the region III mostly stay in place, which indicates that the droplet has a tendency to spread to high-wetting region. The above results confirm that the fabricated gradient wetting surface has the ability to direct the transport of droplets.

Another typical example of heterogeneous wetting surfaces is the extreme wettability contrast surface, which has also received extensive attention due to its efficient water collection performance. The combination of superhydrophilic pattern and superhydrophobic background on the same surface is inspired by Namib desert beetles, and they can collect water from dew and fog using complementary superhydrophilic-superhydrophobic skeleton on their back [32]. Inspired by desert beetles, Wang et al. [33] successfully prepared extreme wettability contrast surfaces on titanium substrate by nanosecond laser irradiation and selective UV irradiation. However, this approach is strongly dependent on the photoresponsiveness of titanium and therefore may be not suitable for MGs. Previous study [34] has shown that the wettability of silicone oil modified aluminium surfaces can transform from superhydrophobicity to superhydrophobicity

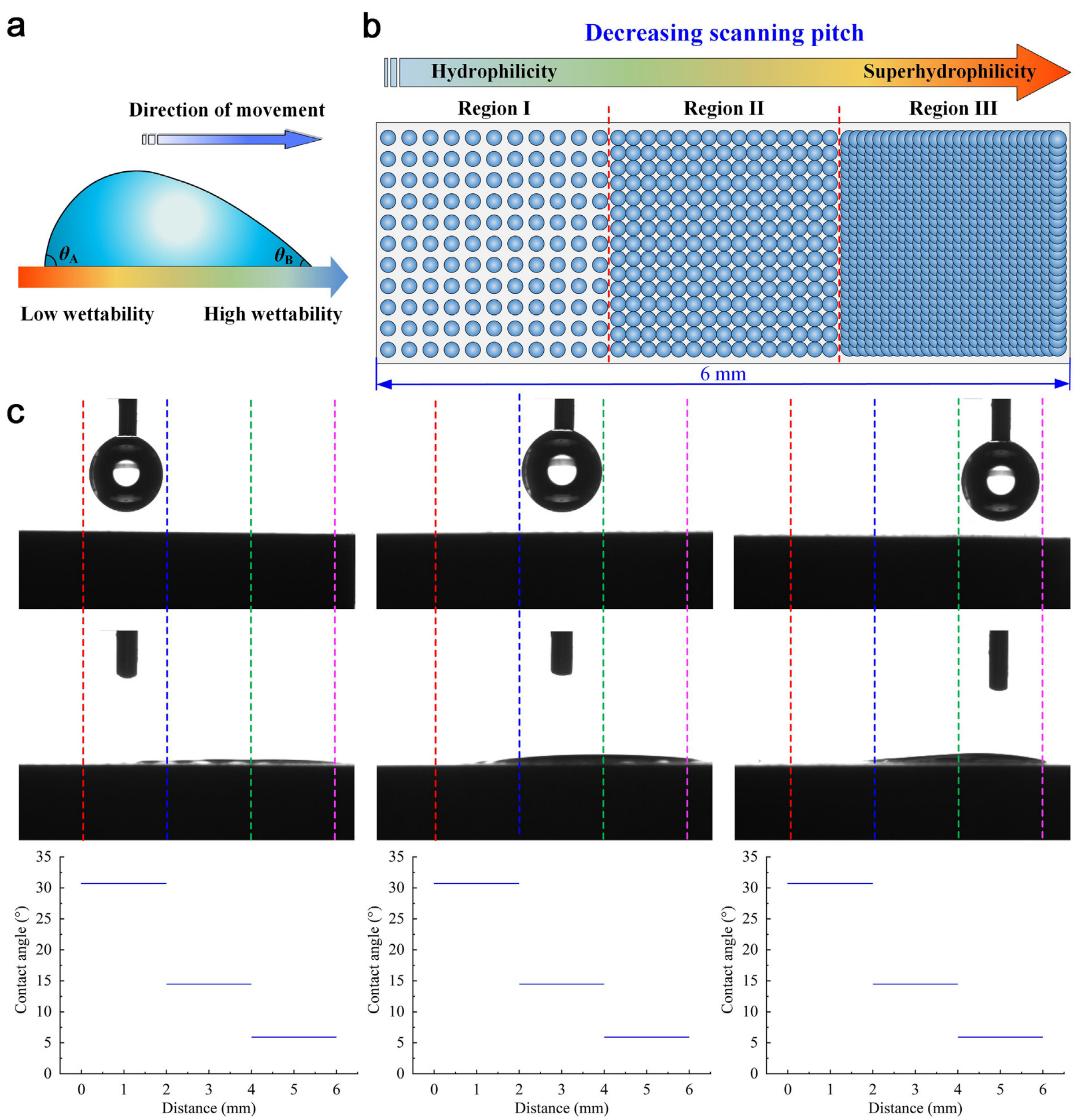


**Fig. 4 – (a) Schematic illustration showing the movement of droplet on the gradient wetting surface. (b) Design diagram of the gradient wetting surface. (c) The final resting positions of droplets dropped on different regions.**

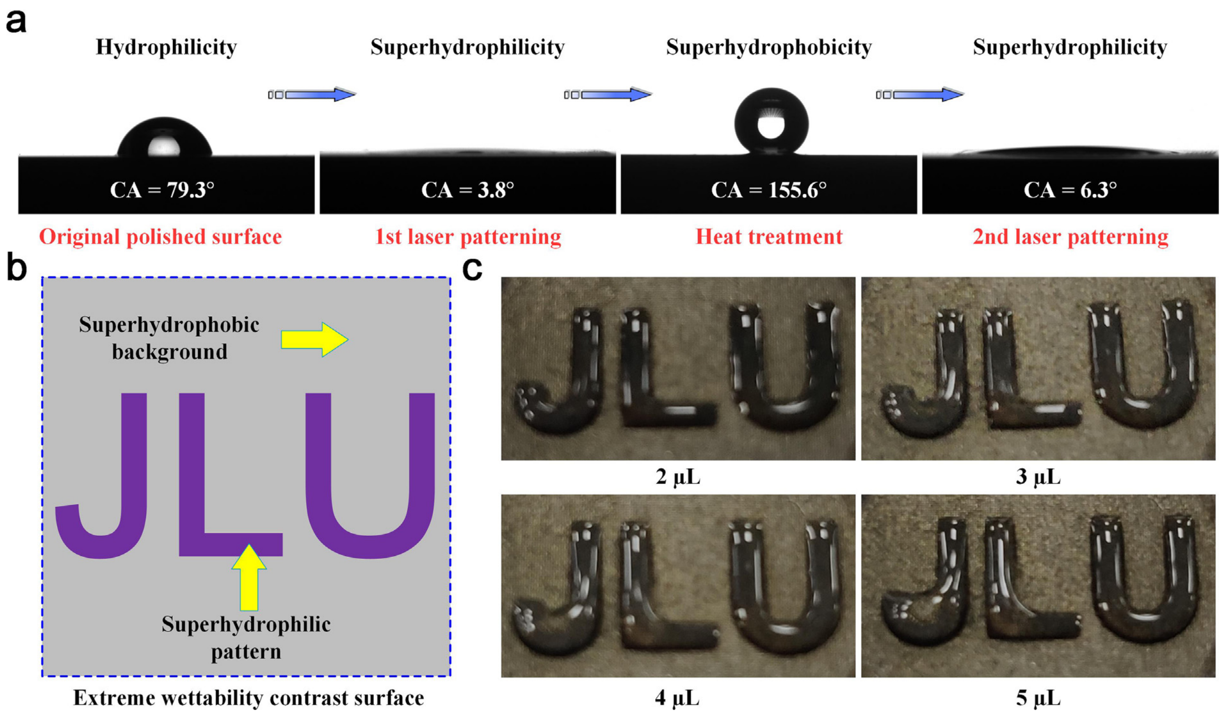


**Fig. 5 – (a) Wettability transition of MG surface after different treatments. (b) Schematic illustration of the constructed extreme wettability contrast surface. (c) Images of superhydrophilic "JLU" patterns filled with deionized water on the heat-treated laser-patterned MG surfaces.**

by laser processing, but the applicability of this method to heat-treated laser-patterned surface remains unknown. To explore the possibility of constructing superhydrophilic patterns on superhydrophobic surface, secondary laser patterning is performed on the heat-treated laser-patterned surface, and the newly laser-patterned surface becomes superhydrophilic again (see Fig. 5(a)). This wettability transition between superhydrophilcity and superhydrophobicity confirms the feasibility of creating flexible superhydrophilic patterns on the heat-treated laser-patterned MG surfaces. Fig. 5(b) presents a schematic illustration of the constructed extreme wettability contrast surface, where the superhydrophilic "JLU" pattern is fabricated by secondary laser patterning, and the other regions retain superhydrophobicity. Fig. 5(c) presents the dispersion of droplets with different volumes falling on the "JLU" pattern. The droplets spread completely according to the designed "JLU" pattern, confirming the good ability of the constructed superhydrophilic-superhydrophobic hybrid wettability surface in controlling the spreading of droplets.

## 4. Conclusions

In this study, laser patterning and low-temperature heat treatment were used to tune the surface wettability of Zr-based MG. The polished MG surface showed hydrophilicity, and it became more hydrophilic after laser patterning, which could be attributed to the increased surface roughness and laser-induced metal oxides. After heat treatment, the hydrophilic laser-patterned surfaces were transformed into hydrophobic ones, and such wettability transition resulted from the adsorption of organic matter mainly including C–C(H) groups from the ambient air. By rationally designing the surface microstructure, a gradient wetting surface was obtained, which could achieve the directional transport of droplets. By performing secondary laser patterning, complex freeform superhydrophilic patterns could be created on the heat-treated laser-patterned surfaces, which exhibited good ability in controlling the spreading of aqueous liquid. This study provides technical guidance for fabricating functional MG surfaces with tailored wettability, which would broaden the practical engineering applications of MGs.

## Declaration of competing interest

The authors declare that they have no known competing financial interests or personal relationships that could have appeared to influence the work reported in this paper.

## Acknowledgements

This work was supported by the Natural Science Foundation of Jilin Province (20220101198JC), the National Natural Science Foundation of China (Grant No. 51705197), the National Outstanding Youth Science Fund Project (No. 12125206) of

NSFC, the Opening Project of the Key Laboratory of CNC Equipment Reliability, Ministry of Education, Jilin University (JLU-cncr-202208), and the Fundamental Research Funds for the Central Universities (2020–2023).

## REFERENCES

[1] Zhou WB, Han DM, Xia GD. Maximal enhancement of nanoscale boiling heat transfer on superhydrophilic surfaces by improving solid-liquid interactions: insights from molecular dynamics. Appl Surf Sci 2022;591:153155.

[2] Yang G, Liu J, Cheng X, Wang Y, Chu X, Mukherjee S, et al. A superhydrophilic metal–organic framework thin film for enhancing capillary-driven boiling heat transfer. J Mater Chem 2021;9(45):25480–7.

[3] Ponsonnet L, Reybier K, Jaffrezic N, Comte V, Lagneau C, Lissac M, et al. Relationship between surface properties (roughness, wettability) of titanium and titanium alloys and cell behaviour. Mater Sci Eng C 2003;23(4):551–60.

[4] Pan R, Zhang HJ, Zhong ML. Triple-Scale superhydrophobic surface with excellent anti-icing and icephobic performance via ultrafast laser hybrid fabrication. ACS Appl Mater Interfaces 2021;13(1):1743–53.

[5] Xing W, Li Z, Yang HO, Li XL, Wang XY, Li N. Anti-icing aluminum alloy surface with multi-level micro-nano textures constructed by picosecond laser. Mater Des 2019;183:108156.

[6] Hwang GB, Page K, Patir A, Nair SP, Allan E, Parkin IP. The anti-biofouling properties of superhydrophobic surfaces are short-lived. ACS Nano 2018;12(6):6050–8.

[7] Zheng YM, Bai H, Huang ZB, Tian XL, Nie FQ, Zhao Y, et al. Directional water collection on wetted spider silk. Nature 2010;463(7281):640–3.

[8] Li N, Xia T, Heng LP, Liu L. Superhydrophobic Zr-based metallic glass surface with high adhesive force. Appl Phys Lett 2013;102(25):251603.

[9] Dumond JJ, Low HY. Long-lasting superhydrophilic polymers via multiscale topographies. ACS Appl Polym Mater 2020;3(1):233–42.

[10] Feng ZJ, Li QH, Wang WW, Ni QK, Wang YF, Song HJ, et al. Superhydrophilic fluorinated polymer and nanogel for high-performance $^{19}F$ magnetic resonance imaging. Biomaterials 2020;256:120184.

[11] Kim S, Cho H, Hwang W. Simple fabrication method of flexible and translucent high-aspect ratio superhydrophobic polymer tube using a repeatable replication and nondestructive detachment process. Chem Eng J 2019;361:975–81.

[12] Wu Y, Cao D, Yao YL, Zhang GS, Wang JY, Liu LQ, et al. Substantially enhanced plasticity of bulk metallic glasses by densifying local atomic packing. Nat Commun 2021;12(1):6582.

[13] Qian YF, Jiang MQ, Zhang ZY, Huang H, Yan JW. On the transformation between micro-concave and micro-convex in nanosecond laser ablation of a Zr-based metallic glass. J Manuf Process 2021;68:1114–22.

[14] Li YS, Wei YP, Yi X, Zhang K, Wei BC. Abnormal change in dynamic mechanical behavior of metallic glass by laser shock peening. Opt Laser Technol 2021;138:106875.

[15] Liu XK, Kong J, Song XX, Feng S, Wang QP, Yang Y, et al. Size dependence of ductile to brittle transition of Zr-based metallic glasses under multiaxial loading. J Mater Res Technol 2021;14:754–64.

[16] Kim SY, Park ES, Eckert J, Lee MH. Role of effective strain on the deformability of brittle Hf-based bulk metallic glass. J Mater Res Technol 2021;15:6713–20.

[17] Wang YY, Wang AM, Li H, Zhang HF, Zhu ZW. The effect of minor alloying on the glass forming ability and crystallization reaction of $Ti_{32.8}Zr_{30.2}Cu_9M_{5.3}Be_{22.7}$ (M=Fe, Co, and Ni) bulk metallic glass. J Mater Res Technol 2022;18:3035–43.

[18] Ford DC, Hicks D, Oses C, Toher C, Curtarolo S. Metallic glasses for biodegradable implants. Acta Mater 2019;176:297–305.

[19] Inoue A, Takeuchi A. Recent development and application products of bulk glassy alloys☆. Acta Mater 2011;59(6):2243–67.

[20] Qian YF, Huang H, Wang C, Yu P, Xu JK, Zhang ZY. Formation of leaf-shaped microstructure on Zr-based metallic glass via nanosecond pulsed laser irradiation. J Manuf Process 2021;72:61–70.

[21] Guo LY, Geng SN, Yan ZC, Chen Q, Lan S, Wang WM. Nanocrystallization and magnetic property improvement of $Fe_{78}Si_9B_{13}$ amorphous alloys induced by magnetic field assisted nanosecond pulsed laser. Vacuum 2022;199:110983.

[22] Qian YF, Huang H, Jiang MQ, Yan JW. Nanosecond pulsed laser-induced formation of nanopattern on Fe-based metallic glass surface. Appl Surf Sci 2022;577:151976.

[23] Wang QH, Gao BT, Raglione M, Wang HX, Li BJ, Toor F, et al. Design, fabrication, and modulation of THz bandpass metamaterials. Laser Photon Rev 2019;13(11):1900071.

[24] Jiao Y, Brousseau E, Shen XJ, Wang XX, Han QQ, Zhu HX, et al. Investigations in the fabrication of surface patterns for wettability modification on a Zr-based bulk metallic glass by nanosecond laser surface texturing. J Mater Process Technol 2020;283:116714.

[25] Cui MM, Huang H, Wang C, Zhang L, Yan JW. Achieving superhydrophobicity of Zr-based metallic glass surfaces with tunable adhesion by nanosecond laser ablation and annealing. ACS Appl Mater Interfaces 2022;14(34):39567–76.

[26] Wang QH, Cheng YY, Zhu ZX, Xiang N, Wang HX. Modulation and control of wettability and hardness of Zr-based metallic glass via facile laser surface texturing. Micromachines 2021;12(11):1322.

[27] Qian YF, Jiang MQ, Zhang ZY, Huang H, Yan JW. Surface functionalization of Zr-based metallic glass by direct nanosecond laser texturing. Vacuum 2021;194:110635.

[28] Ngo CV, Chun DM. Effect of heat treatment temperature on the wettability transition from hydrophilic to superhydrophobic on laser-ablated metallic surfaces. Adv Eng Mater 2018;20(7):1701086.

[29] Li XY, Jiang Y, Tan XY, Zhang ZH, Jiang ZH, Lian JS, et al. Superhydrophobic brass surfaces with tunable water adhesion fabricated by laser texturing followed by heat treatment and their anti-corrosion ability. Appl Surf Sci 2022;575:151596.

[30] Wenzel RN. Resistance of solid surfaces to wetting by water. Ind Eng Chem 1936;28(8):988–94.

[31] Tian Y, Jiang L. Intrinsically robust hydrophobicity. Nat Mater 2013;12(4):291–2.

[32] Zhang JZ, Zhang YC, Yong JL, Hou X, Chen F. Femtosecond laser direct weaving bioinspired superhydrophobic/hydrophilic micro-pattern for fog harvesting. Opt Laser Technol 2022;146:107593.

[33] Wang QH, Wang HX, Zhu ZX, Xiang N, Wang ZD, Sun GF. Switchable wettability control of titanium via facile nanosecond laser-based surface texturing. Surface Interfac 2021;24:101122.

[34] Tran NG, Chun DM. Green manufacturing of extreme wettability contrast surfaces with superhydrophilic and superhydrophobic patterns on aluminum. J Mater Process Technol 2021;297:117245.